Universiteit Utrecht

Opleiding Natuur- en Sterrenkunde

Antiferromagnetic spin waves in a magnetic-field gradient

Bachelor Thesis

R. Wakelkamp

Supervisors:

Prof. Dr. R.A. Duine
Institute for Theoretical Physics

M.Sc. C.E. Ulloa Osorio
Institute for Theoretical Physics

June 12, 2020

Abstract

Recent studies have shown that high levels of ferritin, a type of protein that is found in the brain, could be an indicator of Alzheimer's disease. Therefore it is important to be able to map ferritin in the brain. We hypothesize that this mapping can be done by exciting the spins in ferritin in a way that is similar to nuclear magnetic resonance (NMR). However, unlike the nuclear spins that are excited in NMR, the spins in ferritin are highly coupled due to exchange interactions. We use a one-dimensional antiferromagnetic chain of spins as a model for ferritin. With this model we determine if the application of a linear magnetic-field gradient to such an ensemble of spins results in spin-wave excitations that could be used to image ferritin in the brain. For this purpose, the excitations must be sharply localised in the chain and they should have a distinct frequency. Although we found that there exist excitations that are more narrowly localised due to the magnetic-field gradient, this effect is not found for the large majority of excitations. We also found that the magnetic-field gradient shifts all frequencies up or down by roughly a constant value, meaning the excitations also do not have a distinct frequency. We therefore conclude that this setup is most likely not useful for imaging ferritin.

Contents

1 Introduction **1**

2 Theoretical background **3**
2.1 Heisenberg exchange 3
2.2 External magnetic field 3
2.3 Magnetic anisotropy 4
2.4 Dzyaloshinskii–Moriya interaction 4
2.5 The Landau-Lifshitz-Gilbert equation 5

3 The equilibrium state **6**

4 Deriving the equations of motion **9**

5 Solving the Landau-Lifshitz equation for a constant magnetic field **10**

6 Solving the Landau-Lifshitz equation for a linear magnetic-field gradient **13**
6.1 Effect of the magnetic-field gradient on the frequencies 14
6.2 Effect of the magnetic-field gradient on the localisation of excitations 16

7 Conclusion, discussion and outlook **20**
7.1 Conclusion 20
7.2 Discussion and outlook 20

A Spin waves in a Kagome lattice **22**

1 Introduction

When nuclei with non-zero spin are placed in a magnetic field, their spin will start to precess with a frequency proportional to the applied magnetic field. This precession is called Larmor precession. This effect is the basis of magnetic resonance imaging (MRI). In MRI scanners a linear magnetic-field gradient is applied such that the frequency at which the spin of the nuclei resonate will vary as a function of position. Since the nuclear spins are uncoupled to a good approximation, in other words nucleons of neighbouring atoms do not interact, it is possible to excite nucleons at a specific position by way of tuning the Larmor frequency. In simple terms, by applying a pulse with a specific frequency a particular particle can be excited at the position where the Larmor frequency is equal to the frequency of the pulse. This method of observation is called nuclear magnetic resonance (NMR).

Motivated by a recent discussion with T.H. Oosterkamp, who wants to map ferritin, a type of protein found in the brain, we want to investigate how the electronic spins in one dimensional antiferromagnets behave in a linear magnetic-field gradient.
Mapping ferritin in the brain could be important, as high levels of ferritin in the brain might be related to Alzheimer's disease [1]. In this Thesis, we will will analyze a simple model to see if it is possible to map ferritin by way of the electronic spins in the protein instead of the spin of the nuclei. To do this, we need to be able to create sharply localised excitations of the spins with a distinct frequency, just like in an MRI scanner. Contrary to the nuclear spins, the electronic spins of neighbouring atoms are strongly coupled via exchange and Dzyaloshinskii-Moriya interactions. This coupling leads to the phenomenon of spin waves.

In their book on spin waves, Anil Prabhakar and Daniel Stancil [2] describe spin waves as excitations that exist in magnetic materials. While this description is practical it is not very telling. Disturbances in the magnetic lattice of a crystal can propagate through the lattice as a wave, these waves are called spin waves, and where there are waves, there is interesting physics. In a full quantum mechanical treatment of spin waves, spin waves can be quantized as a quasi-particles called magnons. This is analogous to the more commonly known quantization of lattice-vibrations called phonons.
The theoretical concept of spin waves was first introduced by Nobel laureate Felix Bloch in 1930 [3]. Research in spin waves and their applications, however, properly started taking off around the late eighties, when Albert Fert and Peter Grünberg independently discovered giant magnetoresistance [4]. The giant magnetoresistance turned out to have useful applications in data storage. As a consequence they shared to Nobel prize for their discovery in 2007. The research field in spin currents, including spin waves, and their applications has appropriately been dubbed "spintronics" or "magnonics" [5, 6].
Exploiting spin waves for technological purposes is promising because, unlike in regular electronics, spintronics takes advantage of the spin degree of freedom of the electron instead of its charge. Spin waves propagate through a material without the displacement of the electrons themselves. This is in contrast with electronic signals where the electrons, massive particles, themselves propagate through the material. Therefore spin waves can propagate through a magnetic material free from losses, like Joule-heating, that are associated with electronic currents.

In this Thesis we investigate spin waves in one-dimensional antiferromagnetic ensembles of spins in a linear magnetic-field gradient. This serves as a model for ferritin or any chain-like molecule for that matter. We want to see how a linear magnetic-field gradient influences the frequencies and modes of spin waves in these type of chains by comparing them to the frequencies and modes of spin waves in antiferromagnetic chains in a constant magnetic field. We present a Hamiltonian for the spins in a one-dimensional hematite crystal. We use hematite for our model because it is better understood than ferritin. From this Hamiltonian we derive the equations of motions of the spins by linearizing the Landau-Lifshitz-Gilbert equation. We then make a wave ansatz and solve for the frequencies and modes of these waves numerically. We find that the magnetic-field gradient causes high frequency modes to become more localised as opposed to just applying a constant magnetic field. However most excitations that occur do not behave in this way. Therefore we conclude that the setup we propose is most likely not useful for mapping proteins like ferritin.

The remainder of this Thesis is organized as follows: in Chapter 2, we discuss the four interactions that together make up the Hamiltonian. Subsequently we discuss the LLG equation, which describes the dynamics of spins given a Hamiltonian. In Chapter 3, we determine the equilibrium configurations of the system. In Chapter 4, we compute the equations of motion of the system by linearizing the LLG equation around the antiferromagnetic equilibrium state. In Chapter 5, we calculate the dispersion relation of spin waves in a simplified translationally invariant system. Subsequently, in Chapter 6, we compute the frequencies and modes of spin waves in an antiferromagnetic chain of spin in a linear magnetic-field gradient and compare the results with spin waves in a constant magnetic field. We end in Chapter 7 with a conclusion, discussion and outlook.

2 Theoretical background

In this chapter we discuss the four types of interactions that contribute to the Hamiltonian that we use for our model. These are Heisenberg exchange, external magnetic field, magnetic anisotropy and Dzyaloshinskii–Moriya interaction. We also discuss the Landau-Lifshitz-Gilbert equation. This equation is a semi-classical equation that describes the dynamics of the system given a Hamiltonian. in principle all terms that contribute to the total Hamiltonian can be interpreted quantum mechanically or classically depending on whether we interpret the spins themselves as quantum or classical. In our analysis we treat the spins in a classical manner. This means that instead of a spin being represented by a quantum mechanical operator we treat the spin as a classical vector. This discussion is based on [2, 7, 8].

2.1 Heisenberg exchange

The exchange interaction arises from the spin statistics theorem. Electrons have half integer spin hence wave functions of systems with many electrons must be anti-symmetric under exchange of any two electrons. For certain systems this symmetry condition can be relaxed if an exchange interaction term is added to the Hamiltonian. Many quantum and classical theories of magnetism are based on this interaction. In its most general form the exchange Hamiltonian is given by

$$\mathcal{H} = \sum_{\langle i,j \rangle} J_{ij} \mathbf{S}_i \cdot \mathbf{S}_j. \tag{1}$$

The sum is over all pairs of particles i and j and J_{ij} determines the coupling strength between the different pairs. In our analysis we restrict our-self to the most simple form of the Hamiltonian, with a constant J for all sites and summing over nearest neighbours only, ie,

$$\mathcal{H} = J \sum_{\langle i,j \rangle} \mathbf{S}_i \cdot \mathbf{S}_j. \tag{2}$$

Depending on the sign of J we distinguish between ferromagnets and antiferromagnets. In ferromagnets parallel alignment of the spins is favoured, hence parallel alignment must lower the energy of the system, therefore J must be negative. In antiferromagnets anti-parallel alignment is favoured, hence J must be positive.

2.2 External magnetic field

Although I assume the reader is familiar with the physics of spins in magnetic fields, I will, for the sake of completeness, briefly discuss the fundamentals. From quantum mechanics we know that a magnetic moment is associated with a particle's spin. This relationship between magnetic moment and spin is

$$\boldsymbol{\mu}_s = -\gamma \mathbf{S}, \tag{3}$$

with γ being the gyromagnetic ratio of the particle. In classical electrodynamics the Hamiltonian of a magnetic moment $\boldsymbol{\mu}$ in an external magnetic field $\mathbf{H}$ is

$$\mathcal{H} = \boldsymbol{\mu} \cdot \mathbf{H}. \tag{4}$$

Following the canonical quantisation procedure, we obtain the following Hamiltonian for a spin in an external magnetic field

$$\mathcal{H} = -\gamma \mathbf{S} \cdot \mathbf{H} \tag{5}$$

As the reader might know, solving the Schrödinger equation for this system shows that the expectation value of the spin $\mathbf{S}$ will precess around the direction of the magnetic field with a frequency $\omega = \gamma H$. This is precisely the Larmor precession, like discussed in the introduction.

2.3 Magnetic anisotropy

Most magnetic materials have some sort of magnetic anisotropy. This mean that there is/are one or multiple directions in which the material is easily magnetized. In that case we speak of an easy-axis anisotropy. For our Hamiltonian this means that we need to add a term that lowers the energy of the system if a spin is aligned with the anisotropy direction. We can also have the opposite, the spin pointing in a certain direction costing energy, this is called hard-axis anisotropy. The mechanism behind magnetic anisotropy is spin-orbit coupling and dipole-dipole interactions. Magnetic anisotropy is highly dependent on the geometry of the system. In general magnetic anisotropy is much weaker than the exchange interaction, but because it acts over long length scales it cannot be neglected.
In this Thesis we will consider only easy-axis anisotropy. The Hamiltonian is as follows

$$\mathcal{H} = -\frac{K}{2} \sum_i (\mathbf{S}_i \cdot \mathbf{e})^2. \tag{6}$$

The factor K determines the strength of the anisotropy and the vector $\mathbf{e}$ is a unit vector in the anisotropy direction. In our case it does not matter if the spins are parallel to the anistropy direction or antiparallel.

2.4 Dzyaloshinskii–Moriya interaction

The Dzyaloshinskii-Moriya interaction (DMI) was first introduced by Dyaloshinskii [9] in 1957 as an explanation for weak ferromagnetism found in otherwise antiferromagnetic materials. Later in 1960 Moriya [10] showed that the DMI could be explained by strong spin-orbit coupling in the type of materials in which weak ferromagnetism was observed. The Dzyasloshinskii-Moriya interaction is also known as antisymmetric-exchange. Its Hamiltonian is given by

$$\mathcal{H} = \sum_{\langle i,j \rangle} \mathbf{D}_{ij} \cdot (\mathbf{S_i} \times \mathbf{S_j}) \,. \tag{7}$$

Antisymmetric-exchange acts in a plane. The vector $\mathbf{D}_{ij}$ encodes the strength of the interaction between a pair of spins and is normal to the plane the DMI acts in. It is energetically favourable for spins to align perpendicular to each other in this plane. However, the cross product implies that exchanging a pair of spins will produce the opposite effect, hence the name 'antisymmetric-exchange'. Microscopically, DMI comes from the combined effect of lack of inversion symmetry and spin-orbit coupling.

2.5 The Landau-Lifshitz-Gilbert equation

Consider a single spin $\mathbf{S}$ in a magnetic field $\mathbf{H}$. Its Hamiltonian is given by

$$\mathcal{H} = -\gamma \mathbf{S} \cdot \mathbf{H}. \tag{8}$$

Using Ehrenfest's theorem, we derive the equations of motion for the expectation value of the spin $\mathbf{S}$,

$$\langle \dot{\mathbf{S}} \rangle = \frac{1}{i\hbar} \langle [\mathbf{S}, \mathcal{H}] \rangle = \gamma \langle \mathbf{S} \rangle \times \mathbf{H}. \tag{9}$$

For reasons that may not be obvious we rewrite this equation as

$$\langle \dot{\mathbf{S}} \rangle = -\langle \mathbf{S} \rangle \times \frac{\partial \mathcal{H}}{\partial \mathbf{S}}. \tag{10}$$

This is the basis for the Landau-Lifshitz-Gilbert equation that describes the dynamics of classical spins. The full Landau-Lifshitz-Gilbert (LLG) equation is given by.

$$\dot{\mathbf{S}} = -\mathbf{S} \times \frac{\delta \mathcal{H}}{\delta \mathbf{S}} + \alpha \mathbf{S} \times \dot{\mathbf{S}} \tag{11}$$

The variational derivative of the Hamiltonian plays the role of an effective magnetic field. The last term is a dissipative term called Gilbert damping, with α the damping parameter, which is a dimensionless number much smaller than one. The number of cycles of precession it takes for the magnetization to reach its equilibrium, is given by $1/\alpha$. Gilbert damping is phenomenological and cannot be derived straightforwardly from a Hamiltonian. Without Gilbert damping we refer to the Landau-Lifshitz-Gilbert equation as just the Landau-Lifshitz equation. In the next chapter, we use the Hamiltonian we discussed here to look at the equilibrium states of the system.

3 The equilibrium state

In this chapter we determine the equilibrium states of our Hamiltonian. For our model of a one-dimensional antiferromagnetic chain we consider the following Hamiltonian

$$\mathcal{H} = J\sum_j \mathbf{S}_j \cdot \mathbf{S}_{j+1} - D\mathbf{z} \cdot \sum_j \mathbf{S}_j \times \mathbf{S}_{j+1} - \sum_j \mathbf{H}_j \cdot \mathbf{S}_j - \frac{K}{2}\sum_j (\mathbf{S}_j \cdot \mathbf{z})^2. \tag{12}$$

From left to right, the Hamiltonian consists of exchange interaction, Dzyaloshinskii–Moriya interaction (DMI) acting in the xy-plane, an applied magnetic field and an easy axis anisotropy in the z-direction. For an antiferromagnet, anti-parallel alignment is favoured in the exchange interaction, hence $J > 0$. Dzyaloshinskii–Moriya interaction favours spins to align perpendicular in the xy-plane, hence the DMI vector points in the z-direction. Aligning with the anisotropy direction also causes the energy to decrease, hence $K > 0$. In our analysis, we consider magnetic fields pointing in the z-direction. Furthermore, only nearest neighbour interactions are taken into account.
To determine the equilibrium state we minimize the Hamiltonian. Since minimizing the full Hamiltonian is complicated, we propose two different equilibrium states, the antiferromagnetic state and the spin flop state. A graphical depiction of the antiferromagnetic state and the spin flop state is shown in Figure 1. In the antiferromagnetic state, the spins are oriented parallel to the anisotropy axis, with neighbouring spins aligning anti-parallel to each-other. By applying a magnetic field parallel to the anisotropy axis, the system transitions to the spin flop state, provided the applied magnetic field is strong enough. The remainder of this chapter is dedicated to finding the critical field that characterizes the transition between the antiferromagnetic state and the spin flop state. For simplicity, we restrict our analysis to a system with an applied magnetic field that is constant throughout the chain.

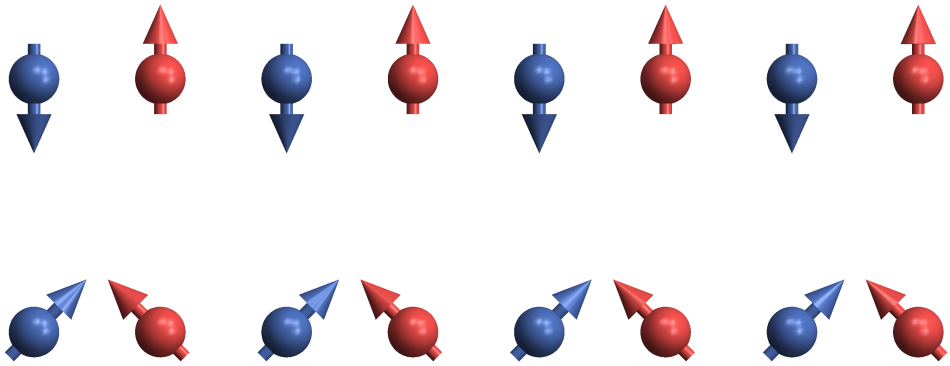

Figure 1: The antiferromagnetic state (top) and the spin-flop state (bottom) in a one-dimensional antiferromagnet.

We divide our lattice into two sub-lattices called A and B such that in the antiferromagnetic state the z-component of all spins in the A lattice is positive and negative for all spins in the B lattice. A neighbouring pair of spins then constitutes a unit cell. Where before we used the index j to indicate a specific spin, we now indicate a unit cell with an index i or j unless stated otherwise, a superscript A/B will denote to which sub-lattice the spin belongs. If we assume periodic boundary conditions then for N spins there are N unique nearest neighbour pairs. The total Hamiltonian of each state is then N times the energy of an isolated unit cell provided we divide H and K by 2 to correct for over-counting. In this setup it is sufficient to look only at the contribution of a single pair to the Hamiltonian since each pair contributes equally. One might make the objection that for the spin-flop state we can have a pair of spins that point towards each-other or away from each-other, however as it turns out the contribution to the Hamiltonian is not affected by the choice of unit cell.
For an isolated unit cell in the antiferromagnetic state, the normalized spin vectors are

$$\mathbf{S}^A = (0, 0, 1)^T, \tag{13}$$
$$\mathbf{S}^B = (0, 0, -1)^T. \tag{14}$$

This amounts to a contribution to the Hamiltonian of

$$\epsilon_{AF} = -J - K/2. \tag{15}$$

For the spin-flop state the normalized spin vectors are

$$\mathbf{S}^A = (\sin\theta, 0, \cos\theta)^T, \tag{16}$$
$$\mathbf{S}^B = (-\sin\theta, 0, \cos\theta)^T, \tag{17}$$

where θ is the angle between the z-axis and the spin vectors. This angle we leave unspecified for now. The energy of this state is

$$\epsilon_{SF} = J\cos 2\theta - H\cos\theta - \frac{K}{2}\cos^2\theta. \tag{18}$$

This is minimised for an angle

$$\theta_m = \arccos\left(\frac{H}{4J - K}\right). \tag{19}$$

Using this result we obtain the following energy for a spin in the spin flop state

$$\epsilon_{SF} = -J - \frac{H^2}{8J - 2K}. \tag{20}$$

To obtain the critical field we solve $\epsilon_{SF} = \epsilon_{AF}$ for the magnetic field H. The critical field that leads to a phase transition between the antiferromagnetic state and the spin flop state is given by the equation

$$H_c = \sqrt{4KJ - K^2}. \tag{21}$$

Because $J \gg K$, we write, to a good approximation, the critical field as

$$H_c = 2\sqrt{KJ}. \tag{22}$$

Below this field the system favours antiferromagnetic ordering and above this field spin flop ordering is favored. A phase diagram is provided in Figure 2. Notice that DMI does not play a role here. This is because the spins are all in the same plane, this plane contains the z-axis and therefore the dot product with the DMI vector and the cross product of two spins vanishes. It is also important to note that this result is not exact for a finite chain in a magnetic-field gradient, but we assume it is an accurate approximation. In this Thesis we will consider spin waves that arise from small deviations away from the antiferromagnetic equilibrium state only. It is therefore important to choose magnetic fields that are below the critical field, since the magnetic field is the only parameter that can be varied experimentally, all the other ones are properties of the material.
Having computed the ground state of the system, we now turn to deriving the equations of motion for small deviations away from the ground state in the next chapter.

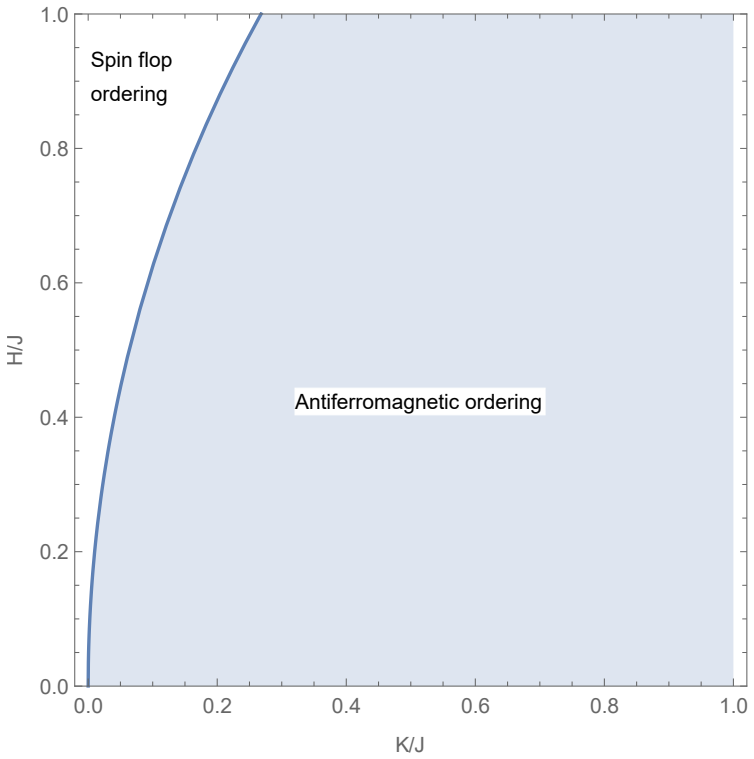

Figure 2: Phase diagram of the antiferromagnetic state and the spin flop state. In the blue region the energy of the system is minimized in the antiferromagnetic state and in the white region the energy is minimized in the spin flop state. The dark blue curve indicates the critical magnetic field.

4 Deriving the equations of motion

In this chapter we compute the equations of motion that follow from the Hamiltonian presented in Eq (12) and the Landau-Lifshitz-Gilbert equation, Eq (11). For the spins we use normalized and dimensionless vectors. The factor of $\hbar$ that spins normally carry, we absorb in the other parameters. As a consequence, to obtain the correct units, we have to divide the effective field in the LLG-equation by $\hbar$. Hence, we have that

$$\dot{\mathbf{S}}_j = -\mathbf{S}_j \times \frac{1}{\hbar}\frac{\delta \mathcal{H}}{\delta \mathbf{S}_j} + \alpha \mathbf{S}_j \times \dot{\mathbf{S}}_j. \tag{23}$$

In the rest of this chapter, we will omit this factor for the sake of notation.
Using the Hamiltonian, we can calculate the effective field acting on each spin. For the spins in the sub-lattice A, the components of the effective fields are

$$\frac{\delta \mathcal{H}}{\delta S_i^{A,x}} = J\left(S_i^{B,x} + S_{i-1}^{B,x}\right) - D\left(S_i^{B,y} - S_{i-1}^{B,y}\right), \tag{24}$$

$$\frac{\delta \mathcal{H}}{\delta S_i^{A,y}} = J\left(S_i^{B,y} + S_{i-1}^{B,y}\right) + D\left(S_i^{B,x} - S_{i-1}^{B,x}\right), \tag{25}$$

$$\frac{\delta \mathcal{H}}{\delta S_i^{A,z}} = J\left(S_i^{B,z} + S_{i-1}^{B,z}\right) - H_i^A - KS_i^{A,z}. \tag{26}$$

For the effective field acting on the spins in sub-lattice B, exchange $A \leftrightarrow B$ and add 1 to each index in the exchange and DMI terms. Now we linearize the LLG equation for small oscillations around the antiferromagnetic equilibrium state, ie, $+z$ for the spins in sublattice A and $-z$ for the spins in sublattice B. These small oscillations around the equilibrium state are known as spin waves. To derive the linearized equations of motion we write the spin vectors as

$$\mathbf{S}_i^A = \left(\delta S_i^{x,A}, \delta S_i^{y,A}, 1 - \left[(\delta S_i^{x,A})^2 + (\delta S_i^{y,A})^2\right]^{1/2}\right)^T, \tag{27}$$

$$\mathbf{S}_i^B = \left(\delta S_i^{x,B}, \delta S_i^{y,B}, \left[(\delta S_i^{x,B})^2 + (\delta S_i^{y,B})^2\right]^{1/2} - 1\right)^T. \tag{28}$$

Expanding everything to linear order in small deviations gives

$$\mathbf{S}_i^A = \left(\delta S_i^{x,A}, \delta S_i^{y,A}, 1\right)^T, \tag{29}$$

$$\mathbf{S}_i^B = \left(\delta S_i^{x,B}, \delta S_i^{y,B}, -1\right)^T. \tag{30}$$

Using this in the LLG equation and keeping terms linear in the deviations only, we find the following equations of motion

$$\delta \dot{S}_i^{A,x} = (2J + H_i^A + K)\delta S_i^{A,y} + J\left(\delta S_i^{B,y} + \delta S_{i-1}^{B,y}\right) + D\left(\delta S_i^{B,x} - \delta S_{i-1}^{B,x}\right) + \alpha \delta \dot{S}_i^{A,y}, \tag{31}$$

$$\delta \dot{S}_i^{A,y} = -(2J + H_i^A + K)\delta S_i^{A,x} - J\left(\delta S_i^{B,x} + \delta S_{i-1}^{B,x}\right) + D\left(\delta S_i^{B,y} - \delta S_{i-1}^{B,y}\right) - \alpha \delta \dot{S}_i^{A,x}, \tag{32}$$

$$\delta \dot{S}_i^{B,x} = -(2J - H_i^B + K)\delta S_i^{B,y} - J\left(\delta S_{i+1}^{A,y} + \delta S_i^{A,y}\right) - D\left(\delta S_{i+1}^{A,x} - \delta S_i^{A,x}\right) - \alpha \delta \dot{S}_i^{B,y}, \tag{33}$$

$$\delta \dot{S}_i^{B,y} = (2J - H_i^B + K)\delta S_i^{B,x} + J\left(\delta S_{i+1}^{A,x} + \delta S_i^{A,x}\right) - D\left(\delta S_{i+1}^{A,y} - \delta S_i^{A,y}\right) + \alpha \delta \dot{S}_i^{B,x}. \tag{34}$$

5 Solving the Landau-Lifshitz equation for a constant magnetic field

In this chapter we use the equation of motion derived in Chapter 4 to find the dispersion of spin waves in a constant magnetic field. We consider a simplified translationally invariant system with periodic boundary conditions. Because the system is translationally invariant under translations of multiples of twice the lattice constant a, we consider the following wave ansatz

$$\delta S_j^{A,x/y} = A_{x/y} e^{ika(2j) - i\omega t}, \tag{35}$$

$$\delta S_j^{B,x/y} = B_{x/y} e^{ika(2j+1) - i\omega t}, \tag{36}$$

k is the wave number and ω the frequency. Using this ansatz, the equation that we have to solve is

$$M \cdot (A_x, A_y, B_x, B_y)^T = 0. \tag{37}$$

With M being the following matrix

$$M = \begin{pmatrix} i\omega & K + H + 2J - i\alpha\omega & i2D \sin ka & 2J \cos ka \\ -K - H - 2J + i\alpha\omega & i\omega & -2J \cos ka & i2D \sin ka \\ -i2D \sin ka & -2J \cos ka & i\omega & -K + H - 2J + i\alpha\omega \\ 2J \cos ka & -i2D \sin ka & K - H + 2J - i\alpha\omega & i\omega \end{pmatrix}. \tag{38}$$

To find non-trivial solutions to this problem the frequency ω must be such, that the determinant of M vanishes. This allows us to find the dispersion relation $\omega(k)$.
To illustrate this, let us consider the simple case where there is no damping and no DMI. In this case the dispersion relation can be determined easily by hand. The result is a follows

$$\omega(k) = \pm H \pm \sqrt{4J^2 \sin^2 ka + K^2 + 4KJ}. \tag{39}$$

The signs in Eq (39) can be chosen separately, hence there are 4 solutions in total. However the $(++)$ and $(--)$ solutions contain the same information, since one is simply the negative of the other. The same goes for the $(+-)$ and $(-+)$ solutions, however, all four solutions are needed to construct real solutions to the linearized LLG equation.
In Figures 3 and 4, we show plots of two examples of the dispersion relation with different parameters. Notice that the frequency is symmetric in ka and is minimal for $ka = 0$. Hence for $H = \sqrt{4KJ + K^2}$ the frequency vanishes at its minimum. However, before we computed that a transition between the antiferromagnetic state and the spin flop state occurs at $H = \sqrt{4KJ - K^2}$. Therefore the spin flop transition occurs before the gap closes in the dispersion relation. If we consider DMI and damping, the analytic solutions to the problem become quite cumbersome, therefore we will not present them here. Instead, we present a numerical solution with DMI but in absence of damping. The absolute value of the numerical solutions is given in Figure 5. We observe that the symmetry, $ka \to -ka$, is broken and that the minimal frequencies are shifted away from 0. DMI typically adds a term linear in k to the dispersion relation, this explains the observations we made before.

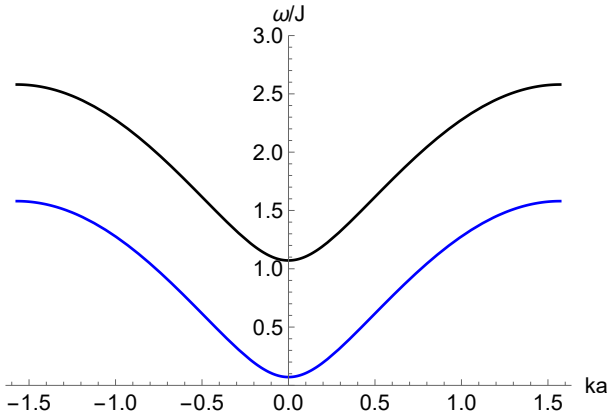

Figure 3: Spin-wave dispersion without DMI. The black line indicates the upper branch and the blue line the lower branch. The magnetic field and anisotropy are respectively, $H/J = 0.5$ and $K/J = 0.08$.

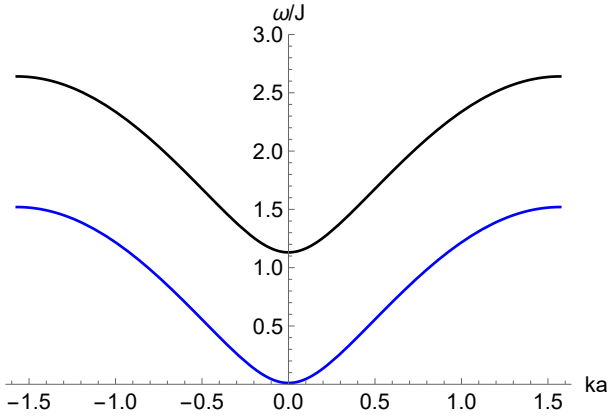

Figure 4: Spin-wave dispersion without DMI at the spin flop transition. The black line indicates the upper branch and the blue line the lower branch. The magnetic field and anisotropy are respectively, $H = \sqrt{4K/J - K^2/J^2}$ and $K/J = 0.08$.

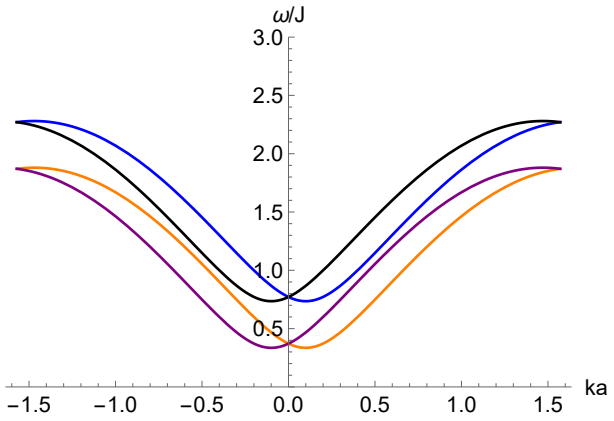

Figure 5: Spin-wave dispersion with DMI. The magnetic field, anisotropy and DMI are respectively, $H/J = 0.2$, $K/J = 0.08$, and $D/J = 0.1$.

6 Solving the Landau-Lifshitz equation for a linear magnetic-field gradient

We have considered an infinite spin chain that is invariant under spatial translations. In this chapter we will consider a spin chain, consisting of N unit cells, in a linear magnetic-field gradient. The gradient in the magnetic field breaks the translational invariance of the system. The linear magnetic-field gradient that we implement has the following form

$$H_j = H_1 - \Delta H \frac{j-1}{2N-1}. \tag{40}$$

Here the subscript denotes a specific spin and not a unit cell. The gradient in the magnetic field, $\Delta H = H_1 - H_{2N}$, is the difference between the magnetic field on the first spin and the last spin. Due to the breaking of translational invariance we have to modify our wave ansatz, disregarding its spatial component. The following ansatz is used to solve the equations of motion

$$\delta S_j^{\mu,x/y} = \mu_j^{x/y} e^{-i\omega t}, \tag{41}$$

where $\mu \in \{A, B\}$, depending on which sub-lattice the spin j belongs to. Now we can construct a matrix equation similar to Eq. (37) with Eqs. (31)-(34). For a system with N unit cells this matrix will be a $4N \times 4N$ matrix. Therefore we will in principle find $4N$ modes. Calculating the null-vectors of this matrix analytically is complicated, therefore we will proceed by calculating the null-vectors numerically.
For our numerical calculation we take 100 unit cells, ie, 200 spins in total and for our model parameters we use $J/\mu_B = 1000$ T , $D/\mu_B = 0.1$ T, $K/\mu_B = 30$ mT, $\alpha = 0$. These are model parameters for a thin film of hematite; hematite is better understood than ferritin. In principle a Gilbert damping of $\alpha = 0.04$ is used for hematite, but neglecting Gilbert damping allows the problem restated as an eigenvalue problem. This allows for much faster computations when considering a system of several hundred spins.
We present results for three different magnetic field gradients. We consider three different values for the magnetic field on the first spin, $H_1 = 1, 5, 10$ T, and linearly decrease to a magnetic field of 0 T on the last spin. This order of magnetic-field strength corresponds to the magnetic-field strengths used in magnetic resonance imaging.

6.1 Effect of the magnetic-field gradient on the frequencies

Since the Heisenberg exchange is large compared to the other parameters we see that the frequency spectra as shown in Figures 6, 7, 8, are for the most part determined by the exchange coupling term. All other parameters give small contributions to the frequency spectra. We find that for every positive frequency there is a corresponding negative frequency, meaning that the complex conjugate of every solution to the LLG equation, also solves the LLG equation. This allows us to construct real solutions to the linearized LLG equation. When we look at the difference between spin waves in a constant magnetic field and spin waves in a magnetic-field gradient, we can make a few observations. First of all, most frequencies are shifted by an amount that is very close to $\pm\Delta H$ with the $\pm$ alternating between each consecutive frequency. At the edges, where the highest frequencies are, we see a more complex pattern but the difference in frequencies are approximately bounded by ΔH on both sides. If we increase the magnetic field gradient the range in which all frequencies are shifted up and down by approximately ΔH gets narrower. There seems to be a transition zone where the shifts decrease/increases linearly until the pattern reaches the other bound, after that it increases/decreases again. At the highest frequencies this pattern seems to break down.

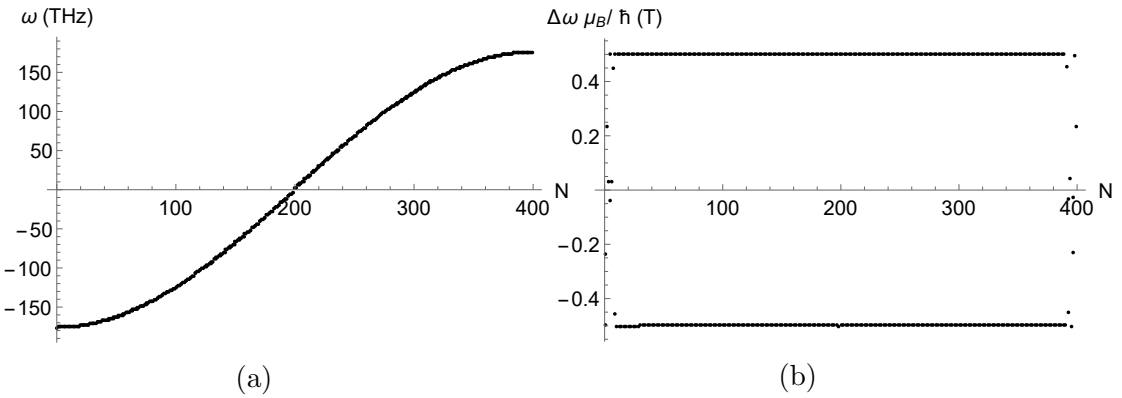

(a) (b)

Figure 6: (a) Frequency spectrum with a magnetic-field gradient of 1 T. (b) The difference between the spectra of spin waves with a constant magnetic field of 1 T and a magnetic-field gradient of 1 T. The frequency difference is in units of tesla. For both (a) and (b), the horizontal axis is there just for book keeping and has no physical meaning

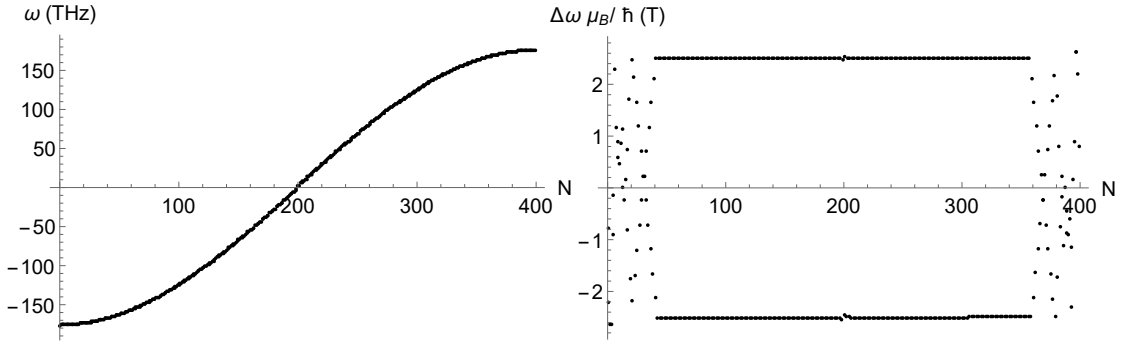

(a) (b)

Figure 7: (a) Frequency spectrum with a magnetic-field gradient of 5 T. (b) The difference between the spectra of spin waves with a constant magnetic field of 5 T and a magnetic-field gradient of 5 T. The frequency difference is in units of tesla. For both (a) and (b), the horizontal axis is there just for book keeping and has no physical meaning

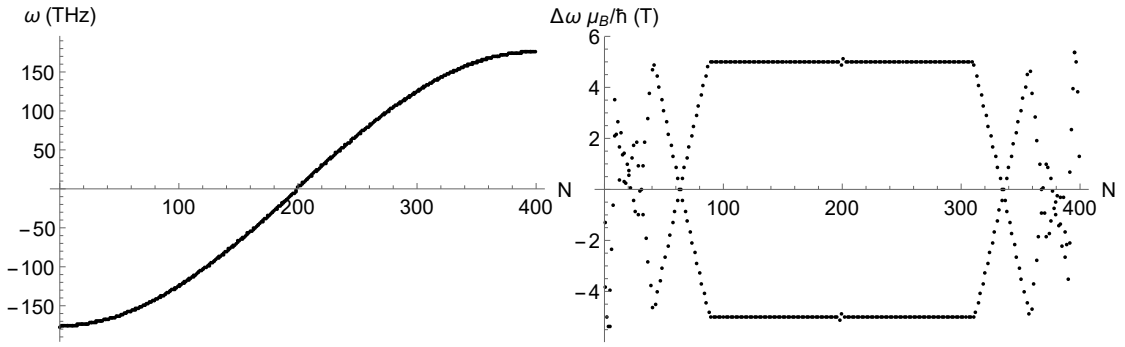

(a) (b)

Figure 8: (a) Frequency spectrum with a magnetic-field gradient of 10 T. (b) The difference between the spectra of spin waves with a constant magnetic field of 10 T and a magnetic-field gradient of 10 T. The frequency difference is in units of tesla. For both (a) and (b), the horizontal axis is there just for book keeping and has no physical meaning.

6.2 Effect of the magnetic-field gradient on the localisation of excitations

Consider a chain of spins that is only affected by a magnetic field in other words we set exchange, damping, anisotropy and DMI to zero. In equilibrium the spins point along the magnetic field, hence the sign of the z-component of a specific spin is equal to the sign of the magnetic field at that specific site. Because there is no interaction between spins the LLG equations decouple. For a single spin the LLG equations of motion simplify to

$$\begin{pmatrix} 0 & H_j \\ -H_j & 0 \end{pmatrix} \begin{pmatrix} \delta S_j^x \\ \delta S_j^y \end{pmatrix} = -i\omega \begin{pmatrix} \delta S_j^x \\ \delta S_j^y \end{pmatrix}. \tag{42}$$

This equation is easily solved, giving the real solutions

$$\begin{pmatrix} \delta S_j^x \\ \delta S_j^y \end{pmatrix} = \begin{pmatrix} \cos[H_j t - \phi_j] \\ \sin[H_j t - \phi_j] \end{pmatrix}, \tag{43}$$

with ϕ_j an arbitrary phase shift. By applying a magnetic field gradient we create a situation where each spin has a distinct frequency. This is in principle what an MRI scanner exploits to make images. We want to investigate the consequences of the presence of exchange and DMI interactions. Since exchange and DMI interactions couple the spins together, we can already conclude qualitatively that the excitations will be dispersed throughout the chain. To illustrate the effects, we look at the localisation of the highest frequencies and lowest frequencies under variation of the exchange parameter. We choose the highest frequency since the higher frequency modes tend to be more localised, the lower frequencies will be more spread throughout the chain. Again we choose magnetic field gradients of 1 T and 10 T.
The results are presented in Figures 9, 10 and 11. For comparison the highest frequency mode for spin waves in a constant magnetic fields are presented in Figure 12.

In the low frequency range we do not observe clear localisation of the excitations around a certain spin or clusters of spins. In fact, the modes are not very different from the modes of spin waves in a constant magnetic field. The shape of the excitations resembles the square of sine waves with different wavelengths. By increasing the frequencies this wavelength gets shorter meaning more wavelengths fit inside the length of the chain. At some point this behaviour breaks down as we can see by looking at high frequencies.
For the high frequencies we find that only the highest frequency is clearly localised around the first spin; on which the highest magnetic field is applied. Cranking up the exchange parameter, we see that the excitation disperses through the chain. The excitation is also mostly present in the A sublattice only. We also observe that the increasing the magnetic field gradient also makes the excitation more narrowly localised on the first spin.

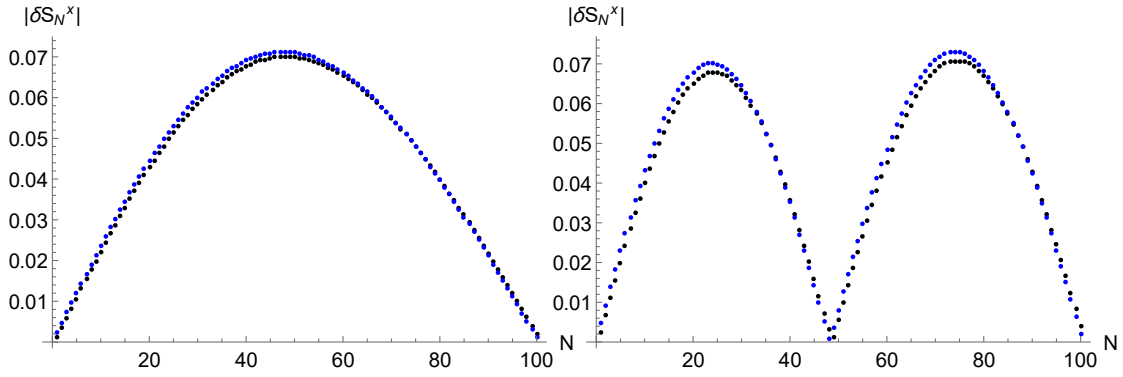

(a) $\omega = 2.46$ THz (b) $\omega = 5.14$ THz

(c) $\omega = 7.86$ THz (d) $\omega = 10.59$ THz

Figure 9: Examples of low frequency modes in a magnetic-field gradient of 10 T. The spins belonging to sublattices A and B are shown in black and blue respectively. The unit cell is on the horizontal axis. The amplitudes are equal in the x and y directions, hence the y-component is not shown

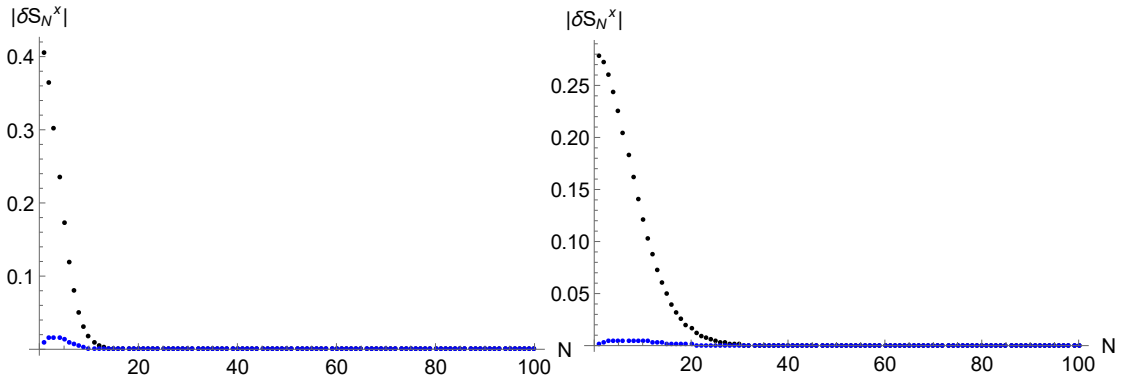

(a) $D/\mu_B = 1/10$ T, $J/\mu_B = 1$ T, $\omega = 0.26$ THz

(b) $D/\mu_B = 1/10$ T, $J/\mu_B = 10$ T, $\omega = 1.84$ THz

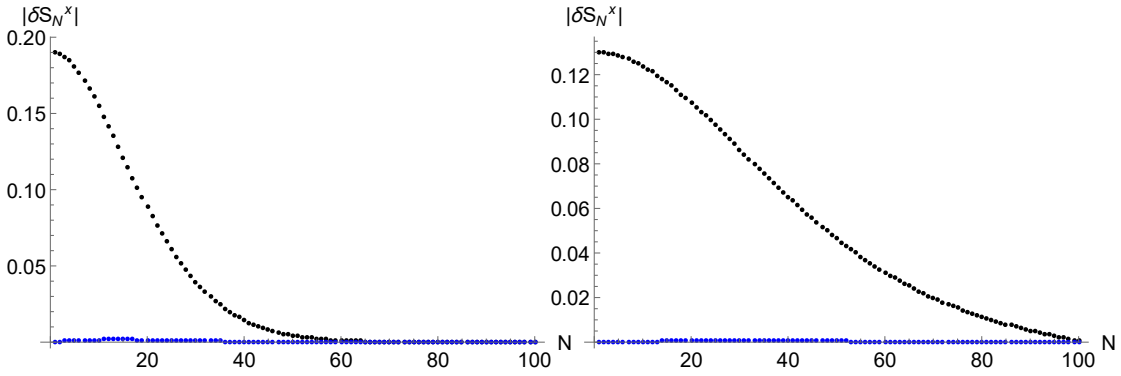

(c) $D/\mu_B = 1/10$ T, $J/\mu_B = 100$ T, $\omega = 17.67$ THz

(d) $D/\mu_B = 1/10$ T, $J/\mu_B = 1000$ T, $\omega = 175.95$ THz

Figure 10: The effect of varying J on the localisation of the highest frequency mode. The magnetic field decreases from 1 T on the first spin to 0 T on the last spin. The spins belonging to sublattices A and B are shown in black and blue respectively. The unit cell is on the horizontal axis. The amplitudes are equal in the x and y directions, hence the y component is not shown.

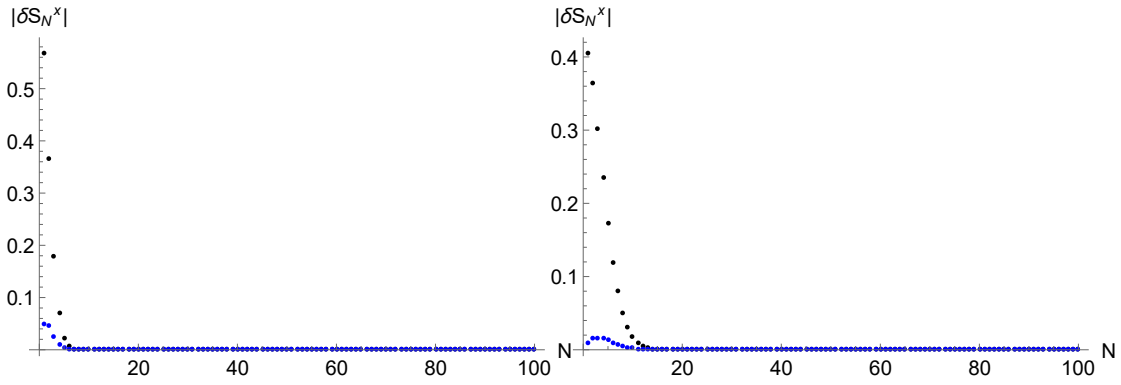

(a) $D/\mu_B = 1/10$ T, $J/\mu_B = 1$ T, $\omega = 1.05$ THz

(b) $D/\mu_B = 1/10$ T, $J/\mu_B = 10$ T, $\omega = 2.62$ THz

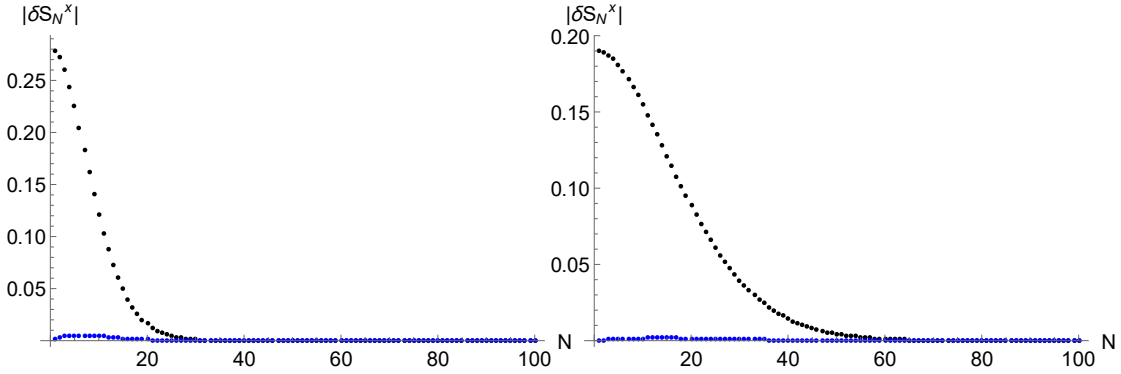

(c) $D/\mu_B = 1/10$ T, $J/\mu_B = 100$ T, $\omega = 18.42$ THz

(d) $D/\mu_B = 1/10$ T, $J/\mu_B = 1000$ T, $\omega = 176.65$ THz

Figure 11: The effect of varying J on the localisation of the highest frequency mode. But with a field decreasing from 10 T on the first spin to 0 T on the last spin.

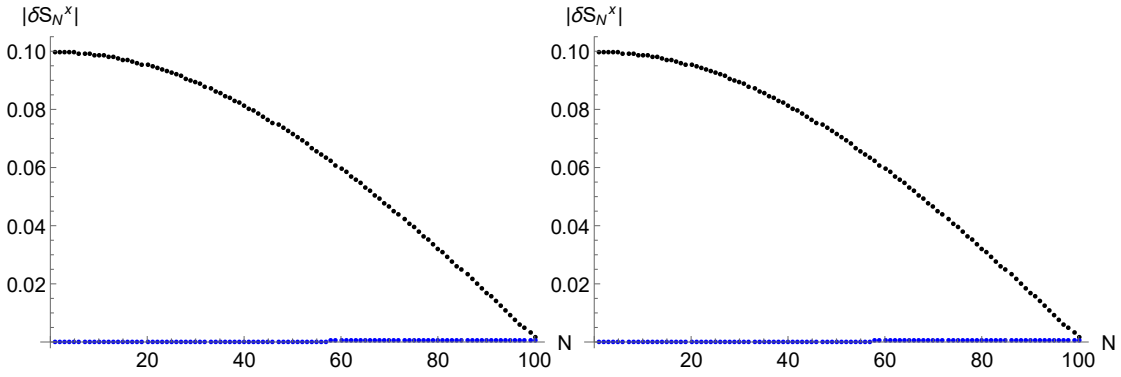

(a) $H/\mu_B = 1$ T, $\omega = 175.97$ THz

(b) $H/\mu_B = 10$ T, $\omega = 176.76$ THz

Figure 12: Localisation of the highest mode for two different constant magnetic fields.

7 Conclusion, discussion and outlook

7.1 Conclusion

The goal of this Thesis was to calculate the spin wave spectrum and modes for an antiferromagnetic chain of spins in a linear magnetic-field gradient, using the Landau-Lifshitz-Gilbert equation. If the spin waves in such a system are well localised and have a characteristic frequency, the spin waves could be used to image chain like molecules like ferritin.
We found that for low frequencies, the frequencies are shifted up or down proportional to half the magnetic field gradient. For high frequencies, we observed more complicated behaviour, but the frequency shifts were still roughly bounded above and below by half the magnetic-field gradient. We observed that for the highest frequency modes, for a few different magnetic-field gradients, the excitations were mostly present in only one of the two sublattices and that the excitations were more sharply localised, in comparison to applying a constant magnetic field on the spin with the highest magnetic field applied. However, we did not observe this for the lower frequency modes. Therefore, we conclude that the excitations of the electronic spins that are found when a magnetic-field gradient is applied, are not suitable for imaging purposes similar to MRI.

7.2 Discussion and outlook

Although we conclude from our calculations that the application of a linear magnetic-field gradient is not sufficient to create excitations that could be resolved positionally, like in an MRI scanner, it does not mean that it is impossible. A glaringly obvious problem is the fact that we had to use model parameters for hematite instead of ferritin. This could in principle make a difference. For instance, depending on the model parameters for ferritin, the critical magnetic field might be much lower for ferritin than it is for hematite. In that case one could look spin waves starting from a different equilibrium state, like the spin flop state. If the coupling terms in ferritin are much smaller compared to the coupling terms of the hematite model, the excitations will presumably be more narrowly localised, as we have seen in this Thesis by varying the exchange coupling.
We used an arbitrary amount of spins for our calculations, in principle this is also a parameter that could be tuned according the spin density in ferritin proteins. Also the geometry of the problem could be improved upon to resemble the structure of ferritin more closely. The structure of ferritin is more complicated than just a chain of atoms. This could for instance affect the number of nearest neighbours.
In this Thesis we used the Landau-Lifshitz-Gilbert equation. This mean we have treated the dynamics of spins semi-classically. For small system, it might also be interesting to consider a fully quantum mechanical treatment of the system. We hope that these suggestions stimulate further research in the imaging of ferritin.

References

[1] P. Kumar, M. Bulk, A. Webb, L. Van Der Weerd, T. H. Oosterkamp, M. Huber, and L. Bossoni, Scientific reports **6**, 38916 (2016).

[2] D. Stancil and A. Prabhakar, *Spin Waves: Theory and Applications* (Springer, 2009), ISBN 978-0-387-77864-8.

[3] F. Bloch, Zeitschrift für Physik **61**, 206 (1930).

[4] M. N. Baibich, J. M. Broto, A. Fert, F. N. Van Dau, F. Petroff, P. Etienne, G. Creuzet, A. Friederich, and J. Chazelas, Physical review letters **61**, 2472 (1988).

[5] A. V. Chumak, V. I. Vasyuchka, A. A. Serga, and B. Hillebrands, Nature Physics **11**, 453 (2015).

[6] V. Kruglyak, S. Demokritov, and D. Grundler, Journal of Physics D: Applied Physics **43**, 264001 (2010).

[7] S. V. Kusminskiy, *Quantum Magnetism, Spin Waves, and Optical Cavities* (Springer, 2019), ISBN 78-3-030-13344-3.

[8] R. Duine, *Spintronics* (Institute for Theoretical Physics, 2010), lecture notes for the course "spintronics", taught at Utrecht University.

[9] I. Dzyaloshinsky, Journal of Physics and Chemistry of Solids **4**, 241 (1958).

[10] T. Moriya, Physical review **120**, 91 (1960).

[11] C. Ulloa and A. Nunez, Physical Review B **93**, 134429 (2016).

A Spin waves in a Kagome lattice

This Appendix will be an extension of work done by C. Ulloa and A.S. Nunez [11]. In [11], the spin dynamics of a noncollinear antiferromagnet with a Kagome lattice geometry are considered. A microscopic classical action is presented. Subsequently, the continuum limit is taken to arrive at a classical field theory. The effective Lagrangian density of this theory is expanded to second order around an equilibrium state. From this expanded Lagrangian density one can obtain the linearized equations of motion of the fields, similar to what we did in this Thesis with the Landau-Lifshitz-Gilbert equation. Our goal is to add Dzyaloshinksii-Moriya interaction (DMI) to the effective Lagrangian density. The results of this Appendix do not directly connect with the previous chapters of this Thesis, that is why it is not included in the main text.

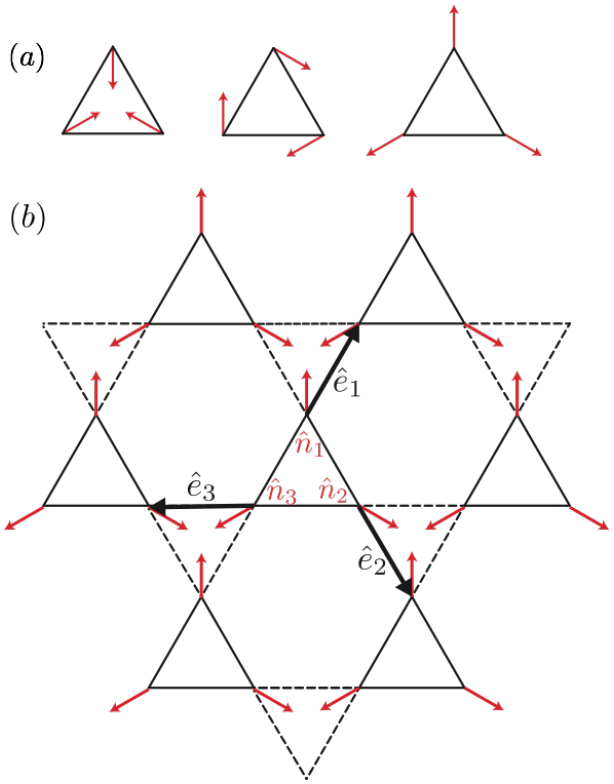

Figure 13: In (a), three different equilibrium states are shown. Here we consider the equilibrium state on the right. In (b) the geometry of the lattice is depicted. The red arrows (labelled $\hat{n}_i$) indicate the spin vectors, while the black arrows are the vectors (labelled $\hat{e}_i$) pointing towards nearest neighbours. The length of the sides of the triangles is given by a. Figure taken from [11].

We represent each spin by a rotation matrix R acting on its corresponding vector $\hat{n}$ and the canting field $\mathbf{L}$, which is assumed to be small,

$$\mathbf{S}_k = R\left(\hat{n}_k + a\left[\mathbf{L} - (\mathbf{L}\cdot\hat{n}_k)\hat{n}_k\right]\right) \tag{44}$$

With this representation we can write the action in terms of the R and $\mathbf{L}$. The DMI contribution to the action in its most general form is

$$\mathcal{S}_{DMI} = -\int dt \sum_{\langle k,m\rangle} \mathbf{D}_{km}\cdot(\mathbf{S}_k\times\mathbf{S}_m)\,. \tag{45}$$

By writing this as a sum over all triangular plaquettes in the lattice, we obtain

$$\mathcal{S}_{DMI} = -\int dt \sum_{\Delta} \mathbf{D}_{13}\cdot\left(\mathbf{S}_1\times\left[\mathbf{S}_3^{+\hat{e}_1}-\mathbf{S}_3^{-\hat{e}_1}\right]\right)+\mathbf{D}_{21}\cdot\left(\mathbf{S}_2\times\left[\mathbf{S}_1^{+\hat{e}_2}-\mathbf{S}_1^{-\hat{e}_2}\right]\right)+\mathbf{D}_{32}\cdot\left(\mathbf{S}_3\times\left[\mathbf{S}_2^{+\hat{e}_3}-\mathbf{S}_2^{-\hat{e}_3}\right]\right). \tag{46}$$

The superscripts $\pm\hat{e}_k$, indicate the location of the nearest neighbour of the spin k. Assuming that changes of the orientation of spins of the same species between neighbouring triangular plaquettes are small, we may write

$$\mathbf{S}_m^{+\hat{e}} - \mathbf{S}_m^{-\hat{e}} = 2a(\hat{e}\cdot\nabla)\mathbf{S}_m. \tag{47}$$

Using this result we obtain

$$\mathcal{S}_{DMI} = -2a\int dt \sum_{\Delta} \mathbf{D}_{13}\cdot[\mathbf{S}_1\times(\hat{e}_1\cdot\nabla)\mathbf{S}_3]+\mathbf{D}_{21}\cdot[\mathbf{S}_2\times(\hat{e}_2\cdot\nabla)\mathbf{S}_1]+\mathbf{D}_{32}\cdot[\mathbf{S}_3\times(\hat{e}_3\cdot\nabla)\mathbf{S}_2]\,. \tag{48}$$

Now we use Eq. (44) to rewrite the action in terms of R and $\mathbf{L}$. Subsequently we take the continuum limit, replacing the sum by an integral,

$$\sum_{\Delta} \to \int dx\, dy \frac{4}{\sqrt{3}a^2}. \tag{49}$$

The resulting action is

$$\mathcal{S}_{DMI} = -\int dt\, dx\, dy \frac{8}{\sqrt{3}a}\epsilon_{ijk}R^{j\alpha}\partial_\beta R^{k\gamma}\left(\Lambda^{i\alpha\beta\gamma}+\mathcal{O}(a^2\mathbf{L})\right), \tag{50}$$

where the tensor $\Lambda^{i\alpha\beta\gamma}$ is defined as

$$\Lambda^{i\alpha\beta\gamma} = D^i_{13}\hat{n}_1^\alpha\hat{e}_1^\beta\hat{n}_3^\gamma + D^i_{21}\hat{n}_2^\alpha\hat{e}_2^\beta\hat{n}_1^\gamma + D^i_{32}\hat{n}_3^\alpha\hat{e}_3^\beta\hat{n}_2^\gamma. \tag{51}$$

We neglect the terms of order $a^2\mathbf{L}$, obtaining the Lagrangian density

$$\mathcal{L}_{DMI} = -\frac{8}{\sqrt{3}a}\epsilon_{ijk}R^{j\alpha}\partial_\beta R^{k\gamma}\Lambda^{i\alpha\beta\gamma}. \tag{52}$$

Because the DMI Lagrangian density does not depend on the canting field $\mathbf{L}$, we can simply add it to the effective Lagrangian density presented in [11]. From here it should be straightforward to compute the dispersion of spin waves.